Excitons in intrinsic and bilayer graphene

Li Yang

Department of Physics, Washington University, St. Louis, Missouri, 63130, USA

(Received 12 November 2010; revised manuscript received 22 December 2010; published 11 February 2011)

Through first-principles calculations with many-body effects included, we have revealed unique excitonic effects in the high-frequency regime (10 $\sim$ 20 eV) of optical spectra of graphene and bilayer graphene (BLG). Despite their different symmetries, the parallel σ and π^* bands result in enhanced excitonic effects in such two-dimensional (2-D) semimetals; one narrowly resonant exciton is discovered to form an isolated peak below the prominent absorption continuum with a surprisingly large binding energy; 270 meV in graphene and 80 meV in BLG. Moreover, because of its extremely weak resonant character, this exciton displays a bound electron-hole wave function and possesses a long intrinsic lifetime, which might be useful in designing optoelectronic applications of graphene.

DOI: 10.1103/PhysRevB.83.085405 PACS number(s): 78.67.Wj, 71.35.Cc, 73.22.Pr

I. INTRODUCTION

Excitonic effects (electron-hole interactions) are known to be of importance to decide the optical response of semiconductors[1] and associated renewable energy applications. Compared with resonant excitons, bound electron-hole (*e-h*) pairs are of peculiar interest because of their well-defined binding energy and much longer life time. For example, the bound exciton generation, diffusion, and annihilation are dictating factors in determining the efficiency of photovoltaic solar cells.[2,3] Despite the great importance of excitons in semiconducting structures, *e-h* interactions had been thought to be negligible in metallic systems and no significant excitonic effect was expected because of their overwhelming metallic screening. However, recent first-principles calculations[4,5] and subsequent experiments[6] have surprisingly confirmed the existence of bound excitons in one-dimensional (1-D) metallic carbon nanotubes (CNTs). Therefore, an obvious question of fundamental interest is whether there is any bound exciton in two-dimensional (2-D) metals or semimetals. The recently fabricated single-layer graphite, graphene,[7–10] is a 2-D semimetal which provides a great opportunity to answer this question.

To date, first-principles calculations[11] and subsequent experiments[12] have revealed enhanced excitonic effects in the optical absorption spectrum of graphene, but those studied excitonic effects resulted from broadly resonant excitonic states consisting of π and π^* bands within the low-frequency regime (up to 10 eV). Because of their dominantly resonant characters, no binding energy can be associated with them and their lifetime is extremely short. All this makes such broadly resonant excitons not very interesting for practical applications.

On the other hand, studies focusing on the higher-frequency regime have revealed enormous red shifts of absorption peaks (3 $\sim$ 4 eV) from the interband transitions between σ and σ^* states,[13] but no reliable and detailed conclusion has been drawn to understand those shifts. In particular, no study has noticed the unique parallel σ and π^* bands in graphene as shown in Fig. 1, although this parallel band structure gives rise to a giant joint density of states (JDOS) and can be of importance for optical activities. Therefore, it is of a fundamental and practical interest for us to focus on excitonic effects in the high-frequency regime of graphene.

In this work, we have calculated the optical spectra of intrinsic graphene and bilayer graphene (BLG) through the GW-Bethe-Salpeter-equation (BSE) approach.[14,15] We first obtain the electronic ground state using density functional theory (DFT)[16,17] within the local-density approximation (LDA); then the quasiparticle excitations are calculated within the GW approximation;[18] finally, we solve the BSE to obtain the photoexcited states and optical absorption spectra.[14,19]

In the high-frequency regime (10 $\sim$ 20 eV), our calculation shows two interesting excitonic effects; broadly resonant excitonic effects substantially reshape the single-particle interband absorption peak but without shifting the absorption edge; below the continuum, one bright narrow resonant exciton emerges. The optical absorption of both types of excitons are comparable, which forms a unique double-peak feature in the corresponding spectrum. This is qualitatively different from those of 1-D metallic CNTs, bulk metals, or semiconductors, in which the continuous optical absorption spectrum is either nearly completely washed out by excitons,[4,5] unchanged, or dominated by resonant excitons.[1,14] Moreover, we show that this narrow resonant exciton has a significant binding energy, long intrinsic lifetime, and bound *e-h* wave functions, so that it can be regarded as a nearly bound state, which is of interest for optoelectronic applications.

The remainder of this paper is organized as follows: in Sec. II, we introduce the calculation details and structure of graphene and BLG; in Sec. III, the quasiparticle band structure of graphene is presented; in Sec. IV, we show the optical absorption of graphene with and without *e-h* interactions included and discuss corresponding excitonic effects; in Sec. V, we show the optical absorption spectra and excitonic effects in BLG; in Sec. VI, we discuss the physical reason for the existence of nearly bound excitons in graphene and BLG; and, in Sec. VII, we summarize our studies and present the conclusion.

II. STRUCTURE AND CALCULATION DETAILS

In our calculations, structures of graphene and BLG are fully relaxed within the DFT/LDA. The plane-wave calculation is done in a supercell arrangement using norm-conserving pseudopotentials[20] with a 60-Ry energy cutoff. The distance

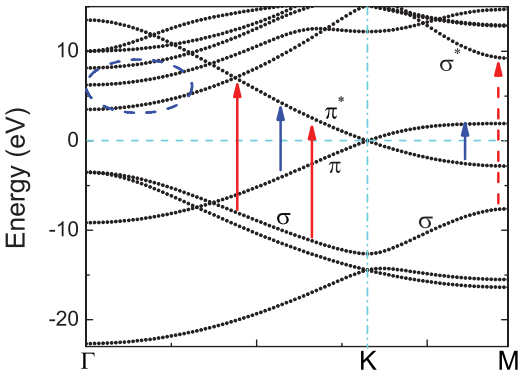

FIG. 1. (Color online) Quasiparticle band structure of graphene. Dashed oval circled bands are nearly free electronic states. The Fermi level is set to be zero.

between neighboring graphene sheets is set to be 2.0 nm to avoid spurious interactions. A $32 \times 32 \times 1$ k-point grid is used to ensure converged LDA results. $64 \times 64 \times 1$ and $128 \times 128 \times 1$ k-point grids are necessary for computing the converged self-energy and optical absorption spectra, respectively. In calculating the self-energy, we have applied the general plasmon pole model to describe the dynamical screening between electrons.[18] When solving the BSE for excitonic effects, we applied the static *e-h* interaction approximation in addition to the Tamm-Dancoff approximation,[14,15] which are both reliable in describing excitonic effects of CNTs, silicon nanowires, and graphene.[4,5,11,21,22] Four valence bands and eight conduction bands are included for optical absorption spectra up to 20 eV for the incident light polarized parallel to the graphene plane. For the incident light perpendicular to the graphene plane, because of the strong depolarization effect, we expect that the corresponding optical absorbance is much weaker.

III. QUASIPARTICLE BAND STRUCTURES

The GW-corrected quasiparticle band structure of graphene is presented in Fig. 1. To date, most works on graphene have focused on interband transitions between π and π^* states,[23–26] which are shown by the blue arrows in Fig. 1. Significant resonant excitonic effects associated with these transitions have been revealed[11] but no bound exciton and associated binding energy have ever been identified within this frequency regime (less than 8 eV).

On the other hand, if σ states are included, bound excitons can possibly be formed. In Fig. 1, there are two types of transitions that could contribute to the formation of potential excitons. The first is transitions between the parabolic σ and σ^* states as marked by dashed red arrows in Fig. 1, which should be well described by the effective mass model and have been noticed by previous works;[13] the other is transitions between parallel σ and π^* bands as marked by solid red arrows in Fig. 1, which have not been studied yet. In particular, the different symmetry of σ and π^* states may introduce novel interband transitions and associated excitonic effects.

IV. OPTICAL ABSORPTION SPECTRUM AND EXCITONIC EFFECTS OF GRAPHENE

The optical absorbance of graphene and BLG is shown in Fig. 2. Within the low-frequency regime (0 to 8 eV), enhanced resonant excitonic effects are predicted and have been identified by experiments.[11,12] Our calculation also shows the identical results as shown in Fig. 2. Moreover, we discover new excitonic effects in the high-frequency regime (above 8 eV), which will be described in the following.

Without *e-h* interactions included, optical absorption spectra of both graphene and BLG show a prominent peak in the high-frequency regime (around $12 \sim 18$ eV) due to the nearly parallel σ and π^* bands and their huge JDOS. The wide broadening of this peak is from the fact that these bands are not perfectly parallel.

Moreover, these parallel bands are of peculiar interest because of their potential enhanced excitonic effects. This parallel dispersion makes it possible for excited electrons and holes to travel together with a similar velocity, which gives hope to enhanced *e-h* pairs. This is a general idea beyond graphene because it is also a critical reason to explain excitonic effects of bulk silicon, an important semiconductor, whose highest valence band and lowest conduction band are largely parallel to each other along the L-Γ-X direction.[1,27] These parallel bands result in significant resonant excitonic effects and weakly bound excitons whose binding energy is around 10 meV in bulk silicon.[19]

After *e-h* interactions are included, the optical absorption spectra of graphene are dramatically changed, as shown in Fig. 2(a). First, a prominent absorption peak shows up below the continuum spectrum at around 12.54 eV. In addition, this absorption peak is robust to different environments and it can survive even for graphene under significant doping conditions.[28] Moreover, our calculation shows that there is

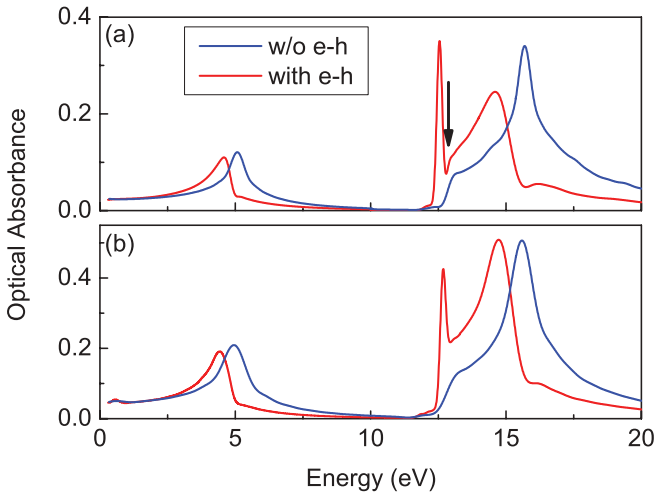

FIG. 2. (Color online) Optical absorption spectra with and without *e-h* interaction included, respectively. Panel (a) shows graphene and (b) shows BLG. The absorbance can be directly compared to experimental measurements.[11] The absorption continuum edge between σ and π^* bands is marked by a black arrow in (a). The absorbance below 0.3 eV is not shown because no Drude factor is included. A 0.08-eV Gaussian broadening is applied.

only one bright excitonic state below the continuum. Since the energy resolution of our calculation in this regime is around 30 meV, we can conclude that the width of this excitonic state absorption profile is much less than this energy resolution, which means it has a really long intrinsic lifetime due to the energy-time uncertainty of quantum mechanics. As a result, this exciton is of peculiar interest for optoelectronic applications.

For such a excitonic state, its binding energy is around 270 meV according to our calculations. Although it is less than than those of narrow semiconducting CNTs and silicon nanowires (SiNWs),[4,5,21,22,29,30] this binding energy is surprisingly large since that of narrow metallic CNTs is only around 30 $\sim$ 50 meV.[4,5] This seems contradictory to the usual idea that higher-dimension materials have weaker excitonic effects. However, the excitons in metallic CNTs consist of only π states while those studied in graphene consists of both σ and π^* states. In this sense, they are different types of excitons and it is inappropriate to compare them in a brute-force way.

On the other hand, in the optical absorption spectrum above the excitonic state, we observe enhanced resonant excitonic effects; the original broad absorption peak is reshaped by these resonant excitonic states, which results in a roughly 1.2-eV redshift of the single-particle absorption peak at around 15 eV. This is similar to what happens in the low-frequency regime (0 $\sim$ 6 eV) of graphene. However, it has to be pointed out that these broadly resonant effects do not move the absorption edge of the continuum as we mark in Fig. 2(a).

After review the optical absorption spectra in Fig. 2(a), an important question is whether this bright excitonic state located at around 12.54 eV is a bound exciton since it is clearly below the prominent absorption edge with a significant binding energy. To better understand this unique exciton, we follow the approach raised by Ref. 11 and rewrite the relevant optical transition matrix element for going from the ground state $|0\rangle$ to an exciton state $|i\rangle = \sum_k \sum_v^{\text{hole}} \sum_c^{\text{elec}} A^i_{vck}|vck\rangle$ in the form[14]

$$\langle 0|\vec{v}|i\rangle = \sum_v \sum_c \sum_k A^i_{vck}\langle vk|\vec{v}|ck\rangle = \int S_i(\omega)\, d\omega, \quad (1)$$

where

$$S_i(\omega) = \sum_{v,c,k} A^i_{vck}\langle vk|\vec{v}|ck\rangle \delta[\omega - (E_{ck} - E_{vk})], \quad (2)$$

which gives a measure of the contribution of all interband pairs (ck, vk) at a given transition energy ω to the optical strength of the exciton state i. In Fig. 3, $S_i(\omega)$ and its integrated value up to a given frequency are presented for two optically bright excited state; one is that prominent exciton whose energy is around 12.54 eV and the other is a broadly resonant excitonic state whose energy is around 13.75 eV.

In Fig. 3, the exciton (a) located in 12.54 eV displays a very different profile from that of the broadly resonant excitonic state (b). Nearly all optical oscillator strength of this exciton is taken from the higher-frequency regime as shown in Fig. 3(a), while the broadly resonant excitonic state takes oscillator strength from both lower- and higher-frequency regimes and exhibits a significant nodal structure across its eigenenergy. In this sense, the prominent exciton is very similar to a bound

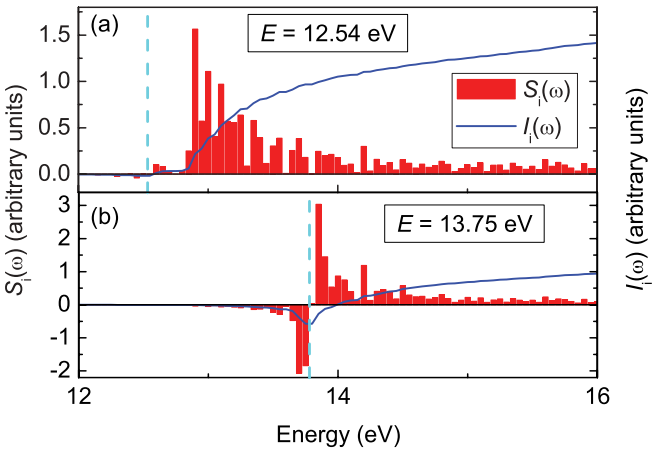

FIG. 3. (Color online) $S_i(\omega)$ and the corresponding integration $I(\omega) = \int_0^\omega S_i(\omega')\, d\omega'$ of two optically bright states in graphene from GW-BSE calculations. Their eigenenergy is marked by dashed cyan lines as well.

exciton. However, if we notice that there is a minor sign change of optical transition matrix elements in this exciton shown in Fig. 3(a) around its eigenenergy (12.54 eV), which implies that this exciton has very tiny resonant components with nearby interband transitions, so it shall be considered strictly as a resonant exciton. According to the integrated value in Fig. 3(a), the resonant component contributes only around 3% of optical activities to this excitonic state. This means this exciton has an extremely narrow resonance and is also consistent with its long intrinsic lifetime.

Moreover, it is known that resonant excitons display delocalized wave functions because of their resonant character. In Fig. 4, we depict the real-space charge distributions of the two bright excitons shown in Fig. 3. As expected, the broadly resonant excitonic state plotted in Fig. 4(b) extends far away and shows an oscillation of the charge distribution. However, the narrow resonant exciton plotted in Fig. 4(a) has a compact envelope function and decays fast away from the hole position, which looks like a bound state. In this sense, this extremely narrow resonant exciton in graphene can be regarded as a nearly bound state.

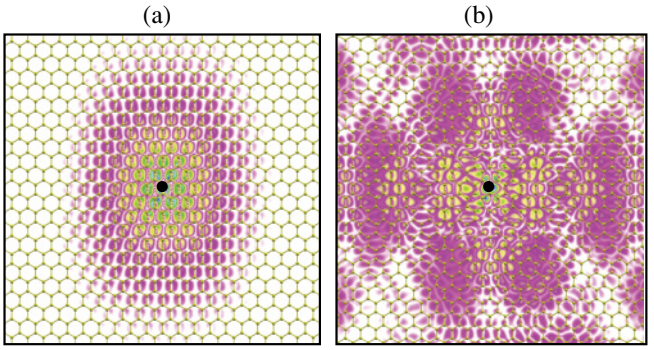

FIG. 4. (Color online) Exciton charge distributions of the two bright exciton states depicted in Fig. 3 for graphene. The electron amplitude squared is plotted, given that the hole is fixed at the black spot. The distributions have been averaged along the direction perpendicular to the graphene plane.

V. OPTICAL ABSORPTION SPECTRUM AND EXCITONIC EFFECTS OF BLG

For AB stacked BLG, we have observed similar excitonic effects; for example, the narrow resonant exciton state is also prominent, as shown in Fig. 2(b). However, due to the stronger screening originated from the parabolic band structure around the Dirac point in BLG, excitonic effects of BLG are weaker. For example, the binding energy of this nearly bound exciton in BLG is around 80 meV, which is roughly one third of that in single-layer graphene. On the other hand, because of the cancellation effect between self-energy and *e-h* interactions,[4,21] frequencies of those two absorption peaks between 12 to 18 eV are roughly the same for both graphene and BLG.

Moreover, the absorbance of this nearly bound exciton state is found to depend on the number of graphene layers. In Fig. 2, the absorbance of the broadly resonant peak (red curve) at around 15 eV of BLG is twice the magnitude of that of graphene, which is reasonable because BLG has two layers involved in the absorption. However, the absorbance of the nearly bound exciton below the continuum in both graphene and BLG is nearly identical. Therefore, when the number of graphene layers increases, the absorption spectrum will be dominated by the broad peak from resonant excitons and it will be hard to detect the nearly bound exciton in many-layer graphene, such as graphite. In this sense, this nearly bound exciton is unique in few-layer graphene.

We have plotted wave functions of the nearly bound exciton and a broadly resonant excitonic state of BLG in Fig. 5. Similar to what has been observed in Fig. 4, wave functions of the nearly bound exciton and the broadly resonant excitonic state are qualitatively different in real-space distributions. Moreover, in Fig. 5(c), if the hole of this nearly bound exciton is located in the upper layer, it has attracted a significant amount of electrons in the lower layer, which reflects the long-range of screened Coulomb interactions in BLG.

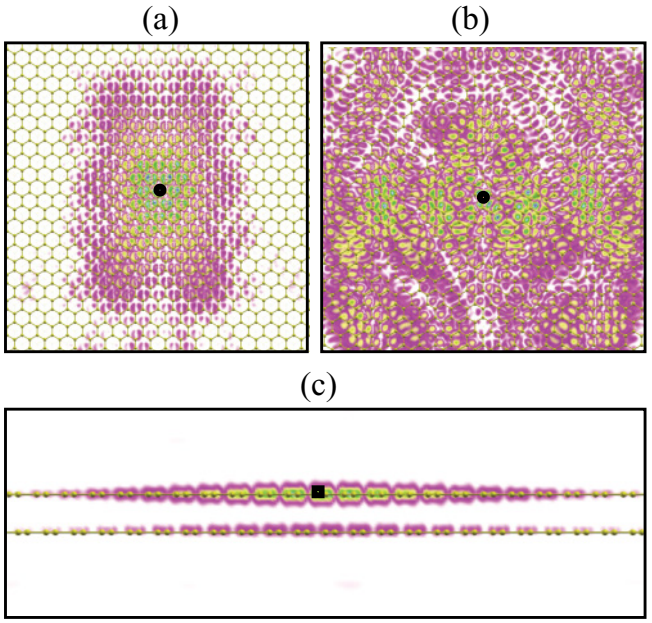

FIG. 5. (Color online) Exciton charge distributions of two bright exciton states in BLG, respectively, with the hole fixed at the black spot. The one plotted in (a) and (c) is the nearly bound exciton located at 12.7 eV and the one plotted in (b) is a resonant exciton located at 14.8 eV. (a) and (b) are the top view and (c) is the side view. These distributions are integrated along the view direction, respectively.

VI. BOUND EXCITONS IN GRAPHENE?

Finally, let us return to the fundamental question, the existence of bound excitons in 2-D semimetals or metals. According to our calculations, no restricted bound exciton can be claimed in graphene and BLG, although there is a nearly bound exciton that has large binding energy and bound *e-h* wave functions. It will be helpful to understand the reason by reminding ourselves of the mechanism to form bound excitons in CNTs. In metallic CNTs, in addition to the reduced dimensionality and depressed screening, an important reason to form bound excitons is the unique symmetry of chiral CNTs, which forms a symmetry gap and prevents the resonant effects between electronic states belonging to different symmetry groups.[5]

For graphene and BLG, they have a reduced dimensionality and depressed screening because the binding energy of the nearly bound exciton is significant. However, the involved σ and π states do not have those chiral symmetries in CNTs, which results in a tiny resonance with nearby single-particle states. Therefore, no pure bound exciton is identified in intrinsic graphene and BLG in our calculation because of the short of a symmetry gap. On the other hand, we do discover that this nearly bound exciton has only extremely narrow resonant components, so that it owns a significant binding energy and bounded *e-h* wave functions. Therefore, this nearly bound exciton will exhibit features similar to the usual bound states and is of importance for practical applications.

VII. SUMMARY

In conclusion, we have performed first-principles calculations on the optical absorption of graphene and BLG. The high-frequency optical spectra are found to be dominated by both broad and narrow resonant excitons. Moreover, we have identified the binding energy of this narrow resonant exciton originated from parallel σ and π^* bands, which is surprisingly large compared to that in narrow metallic CNTs; 270 meV in graphene and 80 meV in BLG. These newly discovered narrow resonant excitons in such a 2-D semimetal exhibits unique features of both optical activity and their charge distributions and are marginal states close to bound excitons, which give rise to optoelectronic applications associated with graphene.

ACKNOWLEDGMENTS

Computational resources are provided by Lonestar of Teragrid at the Texas Advanced Computing Center. The GW-BSE calculation is done with the BerkeleyGW package.

[1]W. Hanke and L. J. Sham, Phys. Rev. B **21**, 4656 (1980); M. del Castillo-Mussot and L. J. Sham, *ibid.* **31**, 2092 (1985).
[2]G. Yu, J. Gao, J. C. Hummelen, F. Wudl, and A. J. Heeger, Science **270**, 1789 (1995).
[3]A. Goetzberger, C. Hebling, and H. Schock, Materials Science and Engineering **40**, 1 (2003), and references therein.
[4]C. D. Spataru, S. Ismail-Beigi, L. X. Benedict, and S. G. Louie, Phys. Rev. Lett. **92**, 077402 (2004).
[5]J. Deslippe, C. D. Spataru, D. Prendergast, and S. G. Louie, Nano Lett. **7**, 1626 (2007).
[6]David J. Cho, Brian Kessler, Jack Deslippe, P. James, Steven G. Louie, Alex Zettl, Tony F. Heinz, and Y. Ron, Phys. Rev. Lett. **99**, 227401 (2007).
[7]K. S. Novoselov, A. K. Geim, S. V. Morozov, D. Jiang, Y. Zhang, S. V. Dubonos, I. V. Grigorieva, and A. A. Firsov, Science **306**, 666 (2004).
[8]K. S. Novoselov, A. K. Geim, S. V. Morozov, D. Jiang, M. I. Katsnelson, I. V. Grigorieva, S. V. Dubonos, and A. A. Firsov, Nature (London) **438**, 197 (2005).
[9]Y. Zhang, Y.-W. Tan, H. L. Stormer, and P. Kim, Nature (London) **438**, 201 (2005).
[10]Zhimin Song, Tianbo Li, Xuebin Li, Asmerom Y. Ogbazghi, Rui Feng, Zhenting Dai, Alexei N. Marchenkov, Edward H. Conrad, Phillip N. First, and A. de Heer, J. Phys. Chem. B **108**, 19912 (2004).
[11]L. Yang, C.-H. Park, J. Deslippe, and S. G. Louie, Phys. Rev. Lett. **103**, 186802 (2009).
[12]V. G. Kravets, A. N. Grigorenko, R. R. Nair, P. Blake, S. Anissimova, K. S. Novoselov, and A. K. Geim, Phys. Rev. B **81**, 155413 (2010).
[13]P. E. Trevisanutto, M. Holzmann, M. Cote, and V. Olevano, Phys. Rev. B **81**, 121405 (2010).
[14]M. Rohlfing and S. G. Louie, Phys. Rev. B **62**, 4927 (2000).
[15]G. Onida, L. Reining, and A. Rubio, Rev. Mod. Phys. **74**, 601 (2002).
[16]P. Hohenberg and W. Kohn, Phys. Rev. **136**, B864 (1964).
[17]W. Kohn and L. J. Sham, Phys. Rev. **140**, A1133 (1965).
[18]M. S. Hybertsen and S. G. Louie, Phys. Rev. B **34**, 5390 (1986).
[19]M. Rohlfing and S. G. Louie, Phys. Rev. Lett. **80**, 3320 (1998); **81**, 2312 (1998); S. Albrecht, L. Reining, R. Del Sole, and G. Onida *ibid.* **80**, 4510 (1998); L. X. Benedict and E. L. Shirley *ibid.* **80**, 4514 (1998).
[20]N. Troullier and J. L. Martins, Phys. Rev. B **43**, 1993 (1991).
[21]L. Yang, C. D. Spataru, S. G. Louie, and M. Y. Chou, Phys. Rev. B **75**, 201304 (2007).
[22]M. Bruno, M. Palummo, A. Marini, R. Del, and S. Ossicini, Phys. Rev. Lett. **98**, 036807 (2007).
[23]R. R. Nair, P. Blake, A. N. Grigorenko, K. S. Novoselov, T. J. Booth, T. Stauber, N. M. R. Peres, and A. K. Geim, Science **320**, 1308 (2008).
[24]Fai Mak, Matthew Y. Sfeir, Yang Wu, Hung Lui, James A. Misewich, and Tony F. Heinz, Phys. Rev. Lett. **101**, 196405 (2008).
[25]C.-H. Park and S. G. Louie, Nano Lett. **10**, 426 (2010).
[26]N. M. R. Peres, R. M. Ribeiro, and A. H. Castro, Phys. Rev. Lett. **105**, 055501 (2010).
[27]M. L. Cohen and J. R. Chelikowsky, *Electronic Structure and Optical Properties of Semiconductors*, 2nd ed. (Springer-Verlag, New York, 1988).
[28]L. Yang (unpublished).
[29]E. Chang, G. Bussi, A. Ruini, and E. Molinari, Phys. Rev. Lett. **92**, 196401 (2004).
[30]F. Wang, G. Dukovic, L. E. Brus, and T. F. Heinz, Science **308**, 838 (2005).